



ELSEVIER

Journal of Atmospheric and Solar-Terrestrial Physics ■ (■■■■) ■■■-■■■

**Journal of  
ATMOSPHERIC AND  
SOLAR-TERRESTRIAL  
PHYSICS**

www.elsevier.com/locate/jastp

# Improvement of global ionospheric VTEC maps by using kriging interpolation technique

R. Orús\*, M. Hernández-Pajares, J.M. Juan, J. Sanz

*Research group of Astronomy & Geomatics/Universitat Politècnica de Catalunya (gAGE/UPC), Modul C3, Campus Nord UPC, c/Jordi Girona 1-3, 08034 Barcelona, Spain*

Received 23 November 2004; received in revised form 11 February 2005; accepted 7 July 2005

## Abstract

In this work, a geostatistic interpolation algorithm, called kriging, has been applied to improve the Technical University of Catalonia (UPC) global ionospheric maps (GIMs) computed with GPS data. This new UPC GIM, from now on UPC kriging GIM, has lower RMS in the observed slant total electron content (STEC) than the current UPC GIM and IGS GIM. Improvements are about 16% and 2%, respectively, using the data of several worldwide distributed GPS stations (self-consistency test). The UPC kriging GIM also presents a better performance than UPC GIM regarding the vertical total electron content (VTEC) measurements from TOPEX/Poseidon and JASON dual-frequency altimetric data. For both standard deviation and RMS, this improvement is about 0.3 TECU (6%) and 0.1 TECU (3%) for TOPEX and JASON, respectively. Moreover, it has also been shown a certain accuracy improvement of the resultant IGS GIM when the UPC kriging GIM replaces the present UPC GIM in the corresponding combination.

© 2005 Elsevier Ltd. All rights reserved.

*Keywords:* Kriging; Total electron content (TEC); Global ionospheric maps (GIMs); GPS; Ionosphere

## 1. Introduction

On June 1998, the International GPS Service (IGS) started an international project to compute different global ionospheric maps (GIMs) on a daily basis by means of using GPS data, see Feltens and Schaer (1998). The centers which have been dealing with that computation, called Ionosphere Associate Analysis Center (IAACs), are: University of Bern (CODE), Energy Mines and Resources (EMR), European

Space Agency (ESA), Jet Propulsion Laboratory (JPL) and Technical University of Catalonia (UPC). During the first three years approximately the different GIMs presented significant total electron content (TEC) biases (Orús et al., 2002) which made difficult to combine them into a common product. Afterwards, several independent updates of techniques carried out by different IAACs made possible to combine the different GIM since they were more compatible. In such scenario, the official *final* combined IGS product started on April 2003, with latencies of about 12 days, having at least the same performance of the best IAACs. Nowadays, a rapid IGS product is being generated with latencies of about 18 h, reaching accuracies only 5–10% worse than the final product, see Hernández-Pajares (2004).

\*Corresponding author. Tel.: +34 93 401 5944; fax: +34 93 401 5981.

*E-mail addresses:* rorus@mat.upc.es (R. Orús), manuel@mat.upc.es (M. Hernández-Pajares), miguel@fa.upc.es (J.M. Juan), jaume@mat.upc.es (J. Sanz).

In this framework, the UPC is developing an interpolation algorithm provided by geostatistics, called kriging, to improve the present UPC GIM. Nowadays, this interpolation technique is useful in a broad fields of applications like mining (Cressie, 1993), hydrology (Samper, 1990), and Earth science, in general (Isaaks and Srivastava, 1989), because it takes into account the spatial correlation among the data to be interpolated. In this context, the kriging technique has been successfully applied in regional VTEC estimation, like Stanislawska et al. (2002), and in getting ionospheric parameters such as near real time FoF2 or M(3000) (Stanislawska et al., 1996). It has been also applied in ionospheric estimation for the wide area augmentation system (WAAS) (Blanch, 2002) and for precise regional ionospheric determination (Wielgosz et al., 2003).

In particular, a method to compute GIMs with kriging interpolation is presented in this work, improving the current UPC and IGS GIMs. This improvement has been tested in two ways. Firstly, the improved accuracy of UPC GIM computed with kriging technique, from now on UPC kriging GIM, has been proved over several GPS stations worldwide distributed, using the so-called self-consistency test, which is applied to get the weights used in the IAAC GIMs combination to get the IGS GIM, see Feltens (2001). This test gives a relative confidence of the different GIM regarding the geometric free carrier phase observation ( $L_1$ ). In this point, the UPC kriging GIM improves the current UPC maps performances in about 16% and about 2% in the IGS GIM. Secondly, an external accuracy test has been performed with altimetric satellite data, such as the TOPEX/Poseidon and JASON satellites, in order to get an absolute accuracy value. In these tests, the UPC kriging GIM has the best performance in both altimeters, reaching an improvement of 6% when it is analyzed with TOPEX data (December 2002, close to solar maximum peak) and about 3% when the JASON data is used (April 2004, at mid decreasing part of the solar-cycle). Finally, it has been also computed the resultant IGS GIM combining the IAACs maps, but replacing the UPC GIM for the UPC kriging GIM. This new IGS GIM shows also slightly better performance than the official IGS GIM. The performance regarding both tests is improved in about 4% (self-consistency) and about 2% (JASON data).

## 2. Basic concepts on kriging technique

### 2.1. Semivariogram estimation

Previously to use the kriging technique it is necessary to determine the semivariogram (or alternatively two-times it, the variogram). This is a function that describes the spatial correlation among the data used in the

interpolation, which knowledge is important since it is used as the main input of the kriging algorithm (6). The semivariogram function is computed by means of doing the squared difference between pairs of observations at a fixed distance  $d_i \pm \Delta d_i/2$ , as it is show in (1), see Cressie (1993) for details:

$$\gamma^*(d_i) = \frac{1}{2m(d_i)} \sum_{i \neq j}^{m(d_i)} (Z_i - Z_j)^2, \quad (1)$$

$\gamma^*$  being the experimental semivariogram,  $m(d_i)$  the number of pairs of observations at a distance  $d_i$ ,  $Z_i$  and  $Z_j$  are the observation values that correspond to points at  $x_i$  and  $x_j$  at a distance  $|x_i - x_j| = d_i$ .

Once the experimental semivariogram is computed, the next step is to adjust this experimental semivariogram to a theoretical one  $\gamma(d_i)$  which must verify several mathematical conditions (Cressie, 1993) in order to be applied in the kriging equations (6). It has to be noted that such theoretical semivariograms are classified in well-known semivariogram *families* which try to take into account the most number of semivariogram types, see Samper (1990) for *families* examples.

### 2.2. Ordinary kriging

The kriging technique is a linear interpolator that belongs to the best linear unbiased estimator (BLUE) family estimators. Thus, the main purpose of the kriging technique is to estimate a certain unknown variable ( $Z^*$ ) as a linear combination of the known values ( $Z_i$ ):

$$Z^* = \sum_i \omega_i Z_i, \quad (2)$$

$\omega_i$  being the weights computed by the kriging equations (6), that are applied to each value  $Z(x_i) = Z_i$ .

In order to apply the *ordinary kriging* technique, it is necessary to assume that the random function  $Z_i$  belongs to the *stationary random functions* family, which means that the mean values and the standard deviation of  $Z_i$  have to be independent of the location. Moreover, the unbiased condition over the weights ( $\sum_i \omega_i = 1$ ) is imposed. Then, the variance is minimized with the help of the Lagrange multipliers in order to impose the unbiased condition, see Cressie (1993) for details:

$$L = \frac{1}{2} E[(Z^* - Z)^2] - \lambda \left( \sum_i \omega_i - 1 \right), \quad (3)$$

$E[(Z^* - Z)^2]$  being the  $Z^*$  variance that can be expressed as a function of the semivariogram:

$$E[(Z^* - Z)^2] = 2 \sum_i \omega_i \gamma_{i0} - \sum_i \sum_j \omega_i \omega_j \gamma_{ij}. \quad (4)$$

After differencing Eq. (3) with respect to  $\lambda$  and  $\omega_i$ , and equating to 0, the *ordinary kriging* equations are

obtained in compact form

$$\sum_i \omega_i \gamma_{ij} + \lambda = \gamma_{i0}. \quad (5)$$

Therefore, in order to get the weights ( $\omega_i$ ), the following equation, that is expressed in matrix notation, has to be solved:

$$\Omega = \Gamma^{-1} \Gamma_0,$$

$$\Omega = \begin{pmatrix} \omega_1 \\ \omega_2 \\ \vdots \\ \omega_n \\ \lambda \end{pmatrix}, \quad \Gamma = \begin{pmatrix} \gamma_{11} & \cdots & \gamma_{1n} & 1 \\ \gamma_{21} & \cdots & \gamma_{2n} & 1 \\ \vdots & \ddots & \vdots & \vdots \\ \gamma_{n1} & \cdots & \gamma_{nn} & 1 \\ 1 & \cdots & 1 & 0 \end{pmatrix},$$

$$\Gamma_0 = \begin{pmatrix} \gamma_{10} \\ \gamma_{20} \\ \vdots \\ \gamma_{n0} \\ 1 \end{pmatrix}, \quad (6)$$

$\Omega$  being the vector that contains the weights  $\omega_i$  and the Lagrange multiplier  $\lambda$ .  $\Gamma$  is the matrix that contains the semivariogram estimations for the *known* values and locations, and  $\Gamma_0$  is the vector that contains the semivariogram estimations for the *unknown* values but with known locations.

### 3. Kriging with GIMs

#### 3.1. Current UPC GIM

Before explaining how to apply kriging technique to GIMs, the current UPC interpolation technique is going

to be briefly explained. In order to calculate the UPC GIMs, the so-called individual vertical TEC is first computed, see Fig. 1 for a distribution example, that is the vertical TEC over each ionospheric pierce point (IPP). This individual vertical TEC, from now on raw TEC, has been computed by means of using a tomographic approach of the ionosphere, which consider that the ionosphere can be described with a 3D voxel model of two layers. With this approximation the mismodelling is reduced when there are large geomagnetic gradients, see Hernández-Pajares et al. (1999) for details. Then, this raw TEC is interpolated using splines functions, see Wessel and Smith (2002), over each IONEX grid point,  $5^\circ \times 2.5^\circ$  in longitude and latitude, and it is smoothed with Gaussian radial basis functions to get the current UPC GIM.

#### 3.2. Data and model

In order to apply the kriging interpolation procedure, the first data choice could be the raw TEC, as it is done with the current UPC GIM, but such TEC field does not verify the condition that its mean value is independent of the location, see Fig. 1 to see an example of the TEC distribution as function of latitude, which is one of the main constrains when the *ordinary kriging* technique has to be applied, see Cressie (1993). In order to overcome this problem, the use of residual data over a model is a more suitable choice, being closer to stationarity hypothesis with constant mean and standard deviation.

Therefore, as a first trial, a planar trend model was adopted to compute the residuals. This model was successfully applied in Blanch (2002) in order to generate ionospheric maps over the United States, but the use of this model is no longer possible due to the fact that in the equatorial zones this planar trend model cannot take into account the equatorial anomalies

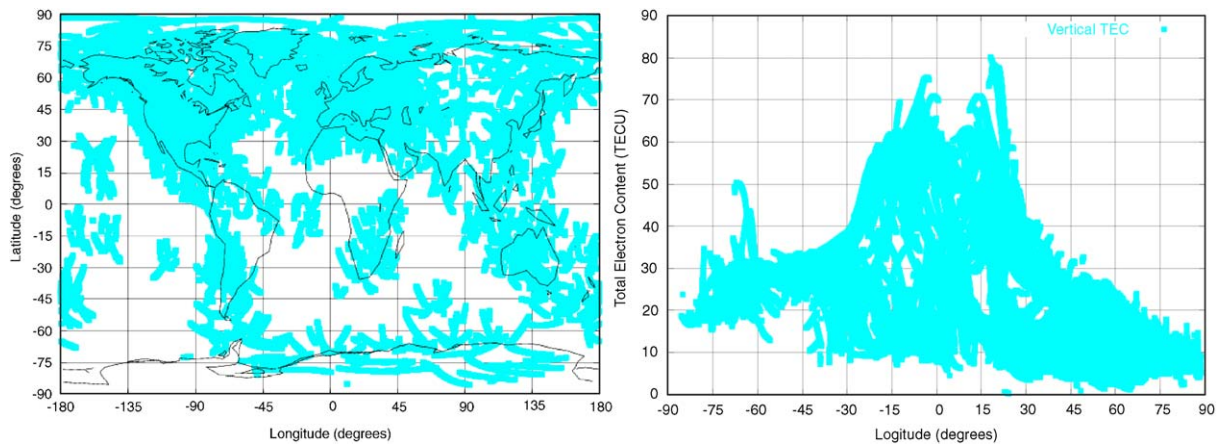


Fig. 1. In the left-hand side plot is depicted the raw TEC pierce points locations. And in the right-hand side plot shows the raw TEC estimations as a function of the latitude. Both plots belongs to the day 3 of January 2003, from 3 to 5 UT.

correctly. Another model used in this work was the International Reference Ionosphere (IRI) model, see [Bilitza \(1990\)](#), but the performance of the final map can be still not so good than the current UPC GIM, see [Table 1](#). Finally, the distributed UPC GIM has been chosen as a base model. This election was due to the fact that the current UPC GIM is the model with the lowest standard deviation over the raw TEC. Indeed, its standard deviation is about 2–3 TECU and the residuals almost fulfill the requirement to be independent of the location, see [Fig. 2](#) for an example. The distributed UPC GIMs also presented the best performance over all the proposed models, see [Table 1](#), using, as it is explained in the next sections, the TOPEX/Poseidon altimeter data. Note that the GIM residuals are obtained interpolating the GIM over each IPP of the raw TEC using the standard interpolation procedure described in [Feltens and Schaer \(1998\)](#).

Table 1  
Bias, standard deviation and RMS (in TECU) of the different kriging approaches and the distributed UPC GIM

| Base model                                   | BIAS | Sigma | RMS |
|--|------|-------|-----|
| <i>TOPEX comparison for January 3rd 2003</i> |      |       |     |
| Planar fit                                   | 2.2  | 4.4   | 4.9 |
| IRI model                                    | 1.8  | 4.5   | 4.8 |
| UPC GIM                                      | 1.8  | 4.1   | 4.5 |
| UPC kriging GIM                              | 1.8  | 3.9   | 4.3 |

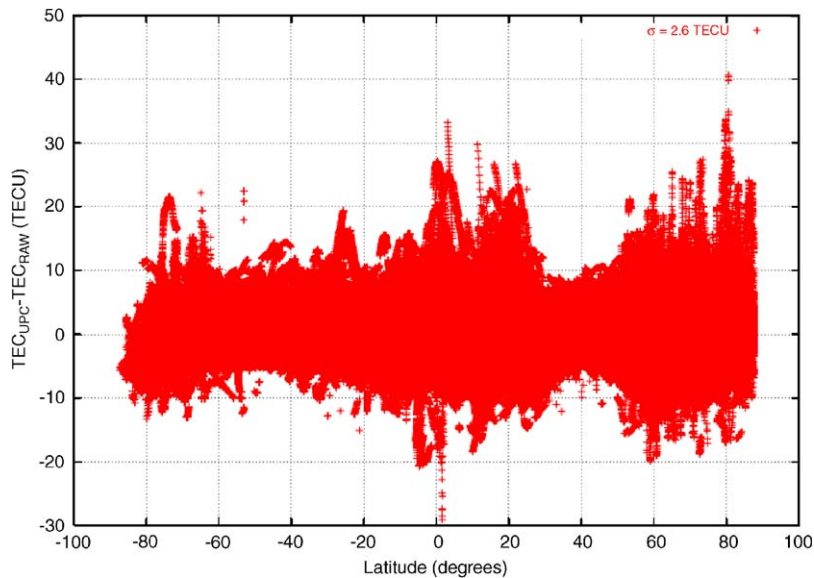


Fig. 2. In this plot there is depicted the residuals of the UPC GIM over the raw TEC data for the day 3 of 2003 for the whole day, the standard deviation is 2.6 TECU and the number of observations is 3,158,292.

### 3.3. Main kriging algorithm

As it has been explained before, the kriging technique requires two main steps when it is applied to interpolation purposes. Once the semivariogram is adjusted, as it will be explained in the next section, the second main step is to solve the kriging equations (6). It is clear that the large amount of data is a drawback since if all the data were taken into account to compute the GIM, a kriging matrix of order  $250,000 \times 250,000$  should be inverted for each map to get the final weights. To overcome this problem, a local strategy is applied for each grid point on the map. For each grid point a local neighborhood of  $45^\circ \times 35^\circ$  in local time and latitude is selected, considering 2 h of data (for instance, centered at 0 UT, 2 UT, and so on). Thus, the problem become inverting 5112 low-order matrix corresponding to each grid point, that in this case ranges from order about  $20 \times 20$  to  $700 \times 700$ , depending on the geographical location. This allows the computation of the kriging weights with less computational time.

The last step is to smooth the final result with a near neighborhood algorithm, see [Wessel and Smith \(2002\)](#) for details, with a spatial domain of  $10^\circ \times 2.5^\circ$  in local time and latitude. With this last step the high-frequency noise is reduced, see [Fig. 3](#) for an example, since the raw TEC is directly used to perform the interpolation.

### 3.4. Semivariogram modelling

As it has been mentioned before, one of the steps to solve the kriging equations is to compute an

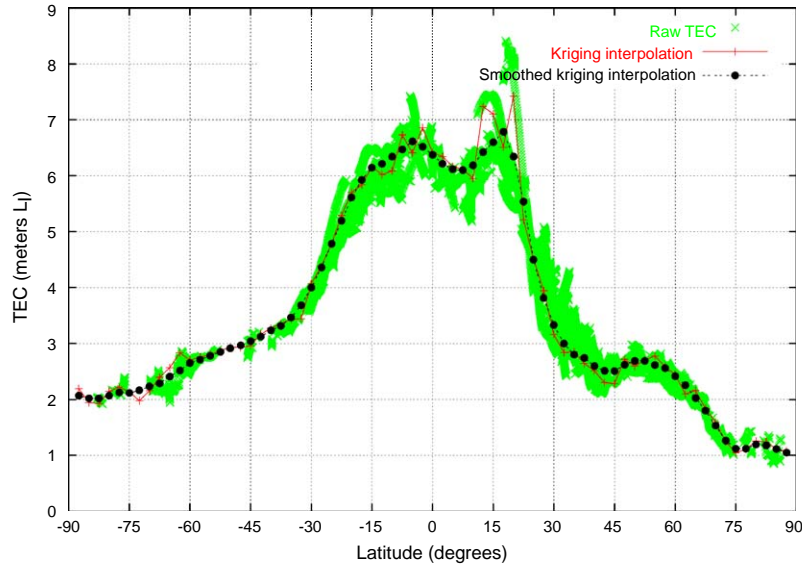


Fig. 3. In this plot the different steps to get a GIM with kriging technique are depicted. In crosses the raw TEC, in lines with crosses the kriging interpolation, after adding the interpolated residual data to the UPC GIM, and in lines with circles the final UPC kriging GIM is represented. This plot corresponds to January 3rd 2003, centered at 4 UT and 185° local time.

experimental semivariogram, in order to adjust a theoretical one. Thus, in principle, one semivariogram should be computed for each realization of the kriging equations (6). This means that when a local strategy is chosen, 5112 semivariograms should be computed, one for each of the  $5^\circ \times 2.5^\circ$  GIM grid points. Such calculation would increase the computation time to undesirable values greater than 24 h for the full processing of a whole day. However, typically the semivariogram normalized by its own mean becomes quite similar (see Fig. 4) and can be adjusted by an exponential function

$$\gamma = a + b(1 - e^{-(x/c)}), \quad (7)$$

$\gamma$  being the adjusted semivariogram,  $x$  the distance between pairs of points, and  $a$ ,  $b$ ,  $c$  the different constants to be computed for each map.

Therefore, for each hourly map, a set of new parameters ( $a, b, c$ ) is obtained which describe the mean behavior of the residuals (see Fig. 5, for an example). These parameters have been obtained computing only some semivariograms worldwide distributed, since as Fig. 4 shows the normalized semivariograms have more or less the same shape. Thus, with only a few number of them it is possible to compute the final semivariogram and the time limit of 24 h is not exceeded.

It is important to mention that the use of just one semivariogram for each hourly map is due to the fact that if a certain constant multiplies the whole semivar-

igram, the weights are not affected as can be deduced from Eq. (5). Therefore, considering only one semivariogram for each 2 h (coinciding with the availability of different maps) is enough.

## 4. Results

In order to quantify the accuracy of the method, several tests have been conducted. The first test provides a relative accuracy of the different GIMs over different GPS receiver data worldwide distributed. This test is called self-consistency test, and it is applied to get the weights that are used to combine the different IAACs GIM in a common IGS GIM.

The second test uses external data to get an absolute accuracy estimate of the different GIMs. In this context, the VTEC data provided by the dual frequency TOPEX/Poseidon and JASON altimeters satellites are used. Both satellites are in a similar orbit at a height above the earth surface of about 1330 km.

### 4.1. GPS data test. Self-consistency test

The self-consistency analyzes the slant ionospheric correction variations along a continuous arch over a single station, see Eq. (8), in such a way that this test provides a measurement of the quality or internal consistency of the STEC computed by

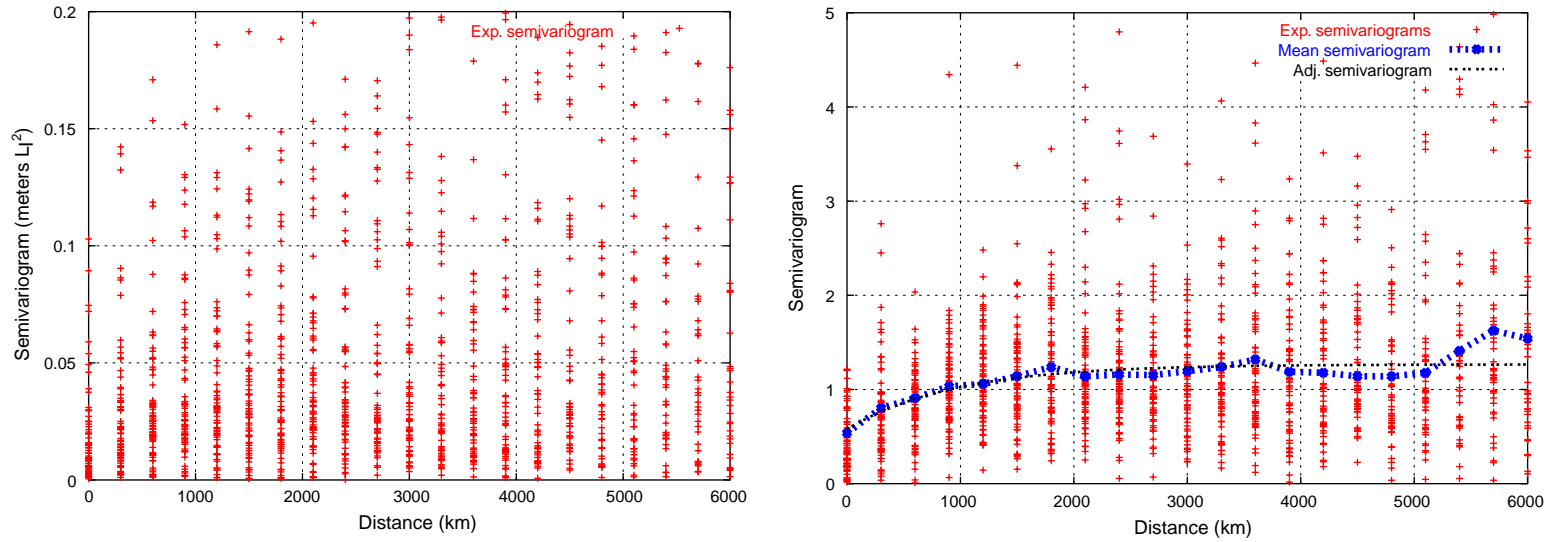


Fig. 4. The left-hand side plot shows the non-normalized semivariogram. And in the right-hand side plot is depicted normalized semivariograms, the mean semivariogram and the adjusted one. Both plots belong to the day of the year (doy) 3 of year 2003 and there is depicted only 2 h interval, from 3 to 5 UT.

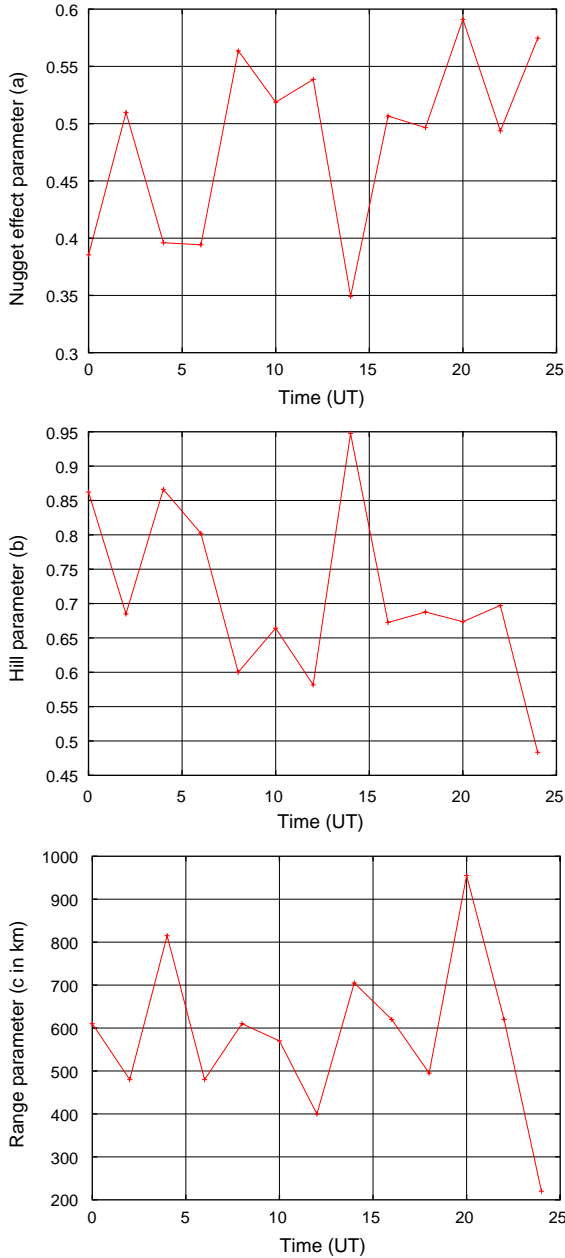


Fig. 5. This figure shows the evolution in time of the different adjusted semivariogram parameters: the nugget effect parameter (top plot), the hill parameter (middle plot) and the range parameter (bottom plot). All of this corresponds to the day 003 of 2003.

each IAACs GIM regarding the very precise carrier phase measurement of the ionospheric refraction  $L_1$ , where

$$L_1 = L_1 - L_2 = STEC + b_1,$$

$$\rho = RMS[L_1(E_{t1}) - STEC_{IAACs}(E_{t1}) - (L_1(E_{t2}) - STEC_{IAACs}(E_{t2}))], \quad (8)$$

$L_1$  being the geometry free combination, the  $STEC$  the Slant TEC, the  $b_1$  is the bias or ambiguity term of the phase observable,  $\rho$  is the RMS of the difference among the  $L_1$  observations and the GIM  $STEC$  prediction at the same elevation  $E$  in a continuous arch taking this difference at two different time, for instance,  $t_1$  and  $t_2$ .

Thus, in Eq. (8) the ambiguity term ( $b_1$ ) of the observation  $L_1$  is canceled in a continuous arch when the two  $L_1$  observations are subtracted. This test is accurate at the level of the phase observable, that has only few millimeters of error noise. Therefore, a very precise test can be conducted with the own GPS data obtaining a relative error of the different IAACs, that is translated in a daily weight. This test is applied over 15 stations worldwide distributed, and then it is computed the global mean RMS.

As it can be seen in Fig. 6, there is an improvement in the UPC performance when the kriging technique is used. Thus, in the period of time from 11th April 2004 to 30th May 2004, the RMS of the UPC kriging map is about 16% lower in mean than the current UPC GIM and about 3% lower than the IGS GIM. Therefore, the kriging GIM fits better the  $L_1$  observable in most of the cases.

#### 4.2. Comparison with altimeter data

This performance number can be obtained computing the bias, standard deviation and RMS regarding TOPEX/Poseidon and JASON altimeters VTEC observations. Such measurements are collected only over the oceans and seas, that is, where few GPS data are available. Thus, such performance study is done on a region where the interpolation method takes special importance since there are no GPS data and the error budget on the GIMs TEC is mainly due to the interpolation process. The use of these two different satellites is justified by the fact that there is non-continuous TOPEX/Poseidon data after the beginning of 2003. Thus, the use of JASON data is required in order to extend the study beyond the year 2003.

##### 4.2.1. Comparison with TOPEX/Poseidon data

In the first altimeter data test, which is conducted with TOPEX data (see Table 2), the UPC kriging GIM is compared with the current UPC GIM, see Fig. 7, for a period of time of 30 consecutive days, starting at the day 335 of 2002. Then, it is also compared with available IGS GIM, during 15 consecutive days, starting at the day 349 of 2002. Note that this period of time is close to the solar maximum peak, with maximum values of TEC compared to other epochs of the solar cycle.

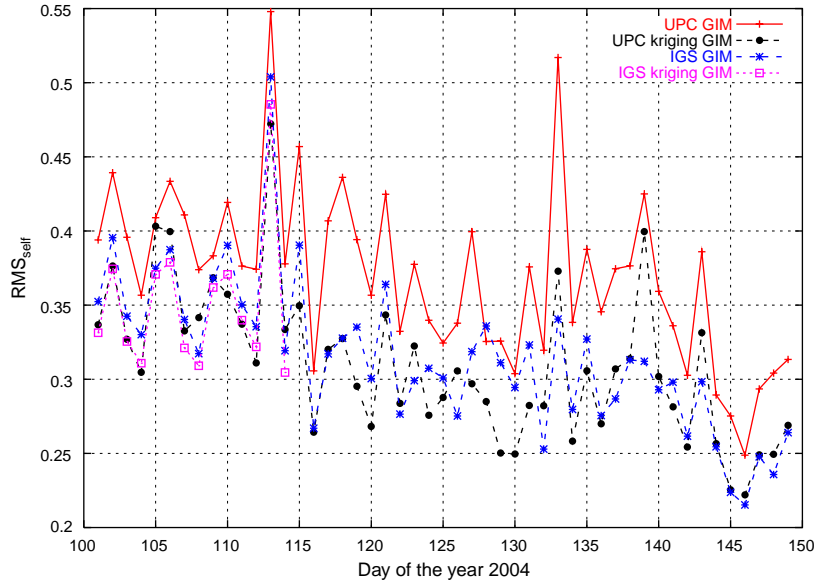


Fig. 6. In this figure it is depicted the mean self-consistency RMS values for each day since 11th April 2004 (GPSweek 1266) corresponding to the different GIMs: UPC, UPC kriging, IGS, IGS kriging.

Table 2

(a) The global bias, standard deviation and RMS (in TECU) of the different GIM models and (b) the latitude band bias and standard deviation of the different GIM model regarding TOPEX data from doy 335 to 365 2002

|  |      | BIAS       |      |            |     | Sigma      |     |            |     | RMS        |     |            |     |            |     |
|--|------|------------|------|------------|-----|------------|-----|------------|-----|------------|-----|------------|-----|------------|-----|
| (a)                                      |      |            |      |            |     |            |     |            |     |            |     |            |     |            |     |
| <i>TOPEX comparison (1,200,000 Obs.)</i> |      |            |      |            |     |            |     |            |     |            |     |            |     |            |     |
| UPC                                      |      | 1.8        |      |            |     | 5.3        |     |            |     | 5.6        |     |            |     |            |     |
| UPC kriging                              |      | 1.8        |      |            |     | 5.0        |     |            |     | 5.3        |     |            |     |            |     |
| IGS <sup>a</sup>                         |      | 0.3        |      |            |     | 5.5        |     |            |     | 5.5        |     |            |     |            |     |
| Lat. band                                | -60° | -40°       | -20° | 0°         | 20° | 40°        | 60° |            |     |            |     |            |     |            |     |
|  | Bi   | $\sigma_T$ | Bi   | $\sigma_T$ | Bi  | $\sigma_T$ | Bi  | $\sigma_T$ | Bi  | $\sigma_T$ | Bi  | $\sigma_T$ | Bi  | $\sigma_T$ |     |
| (b)                                      |      |            |      |            |     |            |     |            |     |            |     |            |     |            |     |
| UPC                                      |      | 1.2        | 4.1  | 0.5        | 4.4 | 1.6        | 6.6 | 2.6        | 6.1 | 3.6        | 7.2 | 1.5        | 2.7 | 2.2        | 2.7 |
| UPC kriging                              |      | 1.4        | 3.7  | 0.8        | 3.9 | 1.7        | 6.0 | 2.2        | 5.9 | 3.1        | 6.9 | 1.8        | 2.5 | 2.5        | 2.5 |
| IGS                                      |      | 1.6        | 4.3  | 0.2        | 4.8 | 0.4        | 5.9 | -1.3       | 6.3 | 0.0        | 7.8 | -0.5       | 3.5 | 1.4        | 3.0 |

<sup>a</sup>From doy 349 to 365 2002.

It can be seen in Table 2 and Fig. 7 that the UPC kriging GIM has better performance, with an improvement of about 0.3 TECU (6% relative error) in standard deviation over the current UPC GIM. And an improvement of about 0.4 TECU (7% relative error) over the combined IGS GIM, with a total of 1,200,000 TOPEX observations. This improvement is not homogeneous in latitude. The most important improvement value is about 10% corresponding to the  $-20^\circ$  of latitude bands

around the south equatorial anomaly. A general improvement can be also observed in all the latitudes bands (see Table 2).

#### 4.2.2. Comparison with JASON data

The second altimeter test, which uses the JASON altimeter VTEC data is summarized in Table 3. The comparison starts at 11th April 2004 and ends at 30th



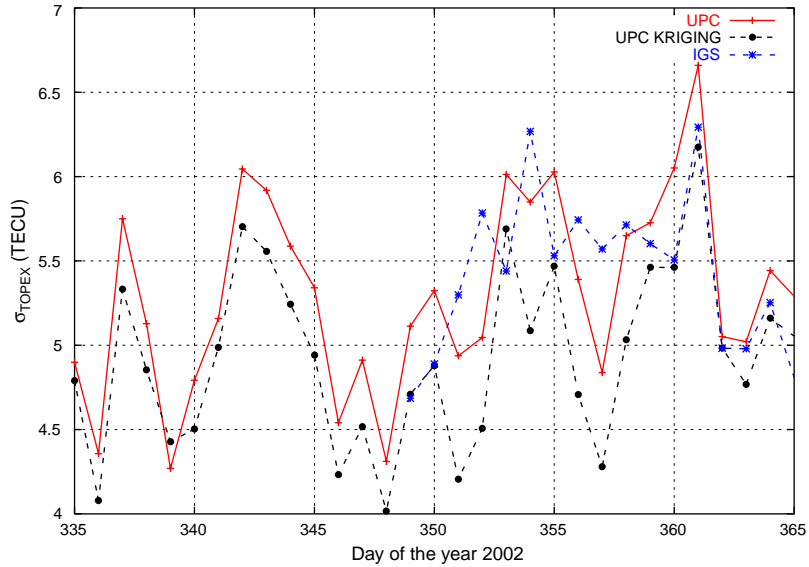


Fig. 7. This plot shows the TOPEX comparison in terms of the standard deviation error among the current UPC GIM, IGS GIM and the UPC kriging GIM, the period studied is 30 days, starting at the doy 335 of 2002. Note that the IGS comparison starts at day 350 of 2002.

Table 3

(a) The global bias standard deviation and RMS (in TECU) of the UPC and IGS GIMs with and without kriging and (b) the latitude band bias and standard deviation of the same GIMs regarding JASON data from doy 102 to 150 2004

|  |      | BIAS       |      |            |      | Sigma      |      |            |      | RMS        |      |            |     |            |
|--|------|------------|------|------------|------|------------|------|------------|------|------------|------|------------|-----|------------|
| (a)                                      |      |            |      |            |      |            |      |            |      |            |      |            |     |            |
| <i>JASON comparison (2,230,000 Obs.)</i> |      |            |      |            |      |            |      |            |      |            |      |            |     |            |
| UPC                                      |      | 0.3        |      |            |      | 3.7        |      |            |      | 3.7        |      |            |     |            |
| UPC kriging                              |      | 0.3        |      |            |      | 3.6        |      |            |      | 3.6        |      |            |     |            |
| IGS                                      |      | -0.2       |      |            |      | 3.9        |      |            |      | 3.9        |      |            |     |            |
| IGS <sup>a</sup> kriging                 |      | 0.0 (-0.1) |      |            |      | 4.0 (4.1)  |      |            |      | 4.0 (4.1)  |      |            |     |            |
| Lat. band                                | -60° | -40°       | -20° | 0°         | 20°  | 40°        | 60°  |            |      |            |      |            |     |            |
|  | Bi   | $\sigma_J$ | Bi   | $\sigma_J$ | Bi   | $\sigma_J$ | Bi   | $\sigma_J$ | Bi   | $\sigma_J$ | Bi   | $\sigma_J$ | Bi  | $\sigma_J$ |
| (b)                                      |      |            |      |            |      |            |      |            |      |            |      |            |     |            |
| UPC                                      | 1.7  | 2.7        | 1.0  | 2.5        | -0.3 | 4.3        | -1.1 | 4.7        | -1.1 | 4.4        | -0.5 | 2.5        | 0.2 | 2.1        |
| UPC kriging                              | 2.2  | 2.5        | 1.1  | 2.5        | -0.3 | 3.9        | -1.5 | 4.6        | -1.1 | 4.0        | -0.5 | 2.3        | 0.3 | 2.1        |
| IGS                                      | 2.4  | 2.4        | 1.3  | 2.6        | -0.7 | 3.6        | -2.9 | 4.9        | -2.5 | 4.1        | -1.0 | 2.5        | 0.8 | 2.2        |
| IGS kriging                              | 2.2  | 2.6        | 1.1  | 2.7        | -0.9 | 4.1        | -2.6 | 5.5        | -1.7 | 4.5        | -0.5 | 2.5        | 1.3 | 2.3        |

<sup>a</sup>In brackets the corresponding values for the IGS GIM from doy 102 to 115.

May 2004, coinciding with the same epoch than the self-consistency test.

As it can be seen in Table 3 and Fig. 8 the UPC kriging GIM has better performance than the current UPC GIM, but in this case the improvement is not as high as in the previous test. In this case, the improvement is about 0.1 TECU (3% in relative error). This may be related to the fact that the TEC in this period is

lower than in the year 2002 (close to solar maximum peak). This fact can produce less correlated residuals. Since the first UPC GIM is accurate enough, the standard deviation regarding JASON altimeter data is 1 TECU lower than the value obtained with TOPEX. Nevertheless, as it has been done with TOPEX/Poseidon data, a latitude band study has been also conducted in order to determine if the improvement is homogeneous.

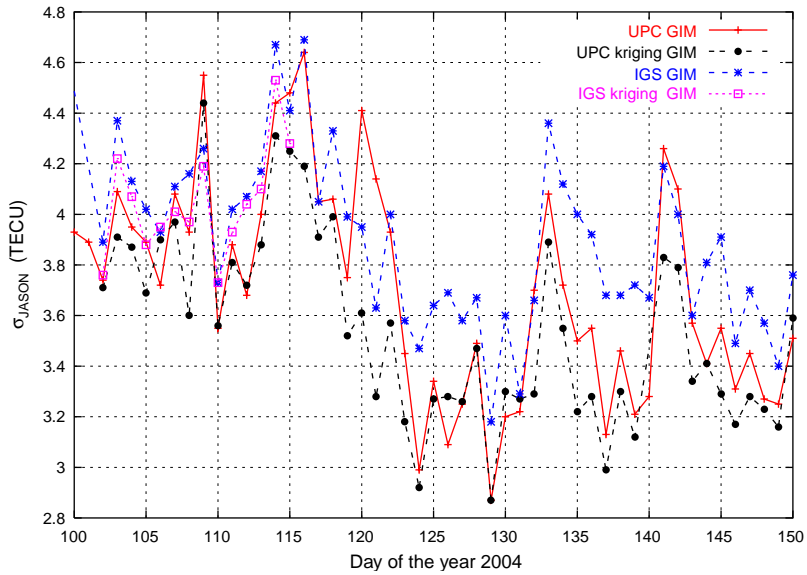


Fig. 8. In this plot there is depicted the JASON comparison in terms of standard deviation error among the current UPC GIM, IGS GIM and the UPC kriging GIM, it is also plotted the IGS GIM obtained with the UPC kriging GIM. The period studied starts at 11th April 2004.

But, looking at Table 3, the most significant improvement corresponds to the  $-20^\circ$  latitude band with a relative error improvement of about 9%. In fact, it seems that the kriging technique improves better in zones with high TEC values. For the remaining latitude bands small improvements or equivalent results are obtained.

#### 4.3. Improving the IGS GIM with kriging

In this section, the IGS GIM has been recomputed using the UPC kriging GIM, instead of the current UPC GIM, in order to quantify the impact of the improvement in the UPC interpolation scheme. As it has been shown above, the UPC kriging GIM presents an improvement of the RMS regarding the self-consistency test. This is important since the self-consistency test provides the weights that will be applied to each IAAC center in order to compute the final IGS GIM. Therefore, the RMS improvement will be translated in an increase weight of the UPC kriging GIM over the other IAACs. The period of time studied comprises from 11th April 2004 to 25th April 2004, and as Table 3 and Fig. 8 show, the error regarding both self-consistency test and JASON altimeter comparison is better, reaching an improvement at the altimeter VTEC of about 4% at latitude band of  $40^\circ$ , when the UPC kriging GIM is used. This is due to the fact that in most of the cases the weight of this new GIM is increased over the other

center about 5% reaching a maximum value of 39% of the total weights (see Fig. 9).

## 5. Conclusions

In this work, the advantages of using the kriging interpolation technique to compute GIMs with GPS data are shown. Several tests have been carried out to analyze the performance of the new UPC kriging GIM in front of the different GIMs available at IGS such as the current UPC and the common IGS maps. For all the tests, the UPC kriging GIM has provided a better performance, improving the UPC GIM of about 12% in the self-consistency test, that it is performed with the use of the worldwide GPS test stations. When, an external source of TEC data is used to compare the absolute accuracy of the UPC kriging GIM, an improvement of about 6% over the old UPC GIMs are achieved. However, when the JASON data is taken into account such improvement is not as high as when the TOPEX data is used at solar maximum conditions, in this case the improvement is about 2%. These results strongly suggest that the use of the kriging technique in global ionospheric mapping is convenient to improve accuracy and smoothness. Additionally, the same test has been applied to the common IGS GIM and to a combined IGS map produced with the UPC kriging GIM, showing that the performance of the IGS kriging GIM is better

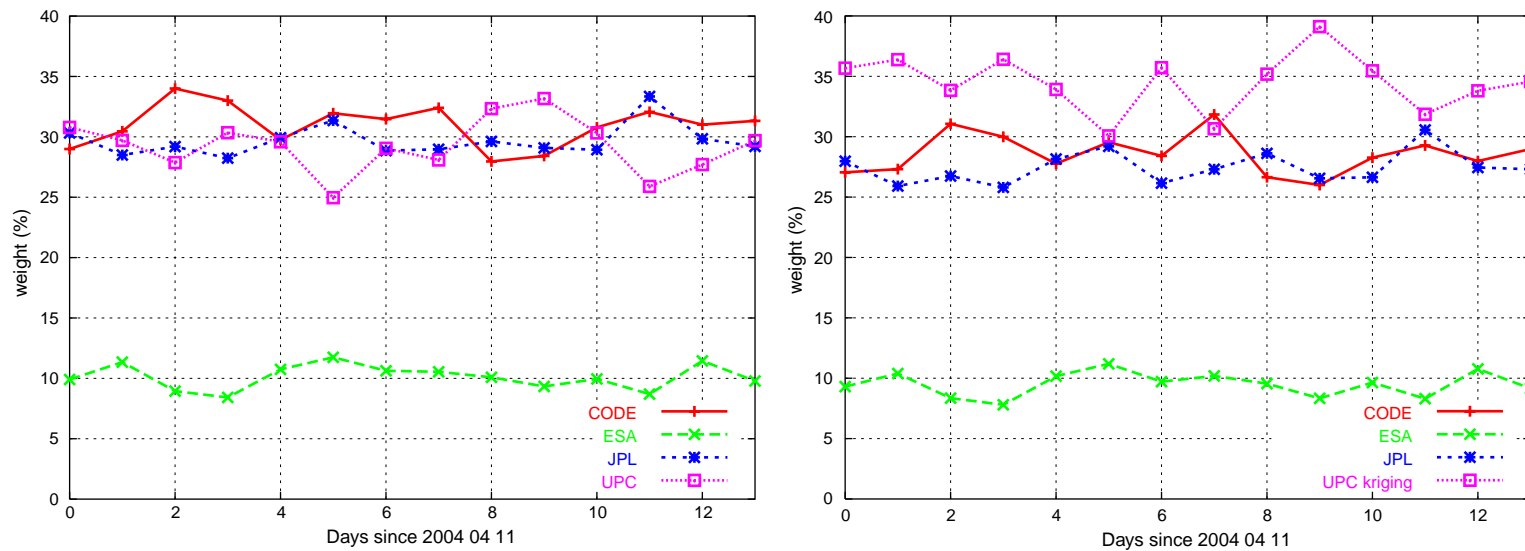


Fig. 9. In the left plot it is depicted the different IAACs daily weights. In the right plot the UPC GIM has been changed by the UPC kriging GIM and it is also depicted the different GIMs daily weights. Both plots start at 11th April 2004 (GPSweek 1266).

than the common IGS product. In this case, the new IGS GIM present a slight improvement over the current IGS GIM (about 2.5% in terms of absolute accuracy).

### Acknowledgements

The GIMs computed by IAACs were obtained from the International GPS Service, IGS. This work has been partially supported by the Eurocontrol contract no. C/1.057/CE/JR/03 and Spanish projects PTR1995-0752-OP and ESP2004-05682-C02-01.

### References

- Bilitza, D., 1990. International reference ionosphere 1990. URSI/COSPAR, NSSDC/WDC-A-R&S 90-22.
- Blanch, J., 2002. An ionosphere estimation algorithm for WAAS based kriging. ION'2002.
- Cressie, N.A.C., 1993. Statistics for Spatial Data, revised ed. Wiley, New York, EUA.
- Feltens, J., 2001. The International GPS service (IGS) Ionosphere working group. The International Beacon Satellite Symposium.
- Feltens, J., Schaer, S., 1998. IGS products for the ionosphere. Proceedings of the IGS Analysis Center Workshop, ESA/ESOC Darmstadt, Germany, pp. 225–232.
- Hernández-Pajares, M., 2004. IGS Ionosphere WG: an overview. Invited presentation at COST271 Action Final Meeting, Abingdon, UK, 26 and 27 August 2004.
- Hernández-Pajares, M., Juan, J.M., Sanz, J., 1999. New approaches in global ionospheric determination using ground GPS data. Journal of Atmospheric and Solar-Terrestrial Physics 61, 1237–1247.
- Isaaks, E.H., Srivastava, R.M., 1989. Applied Geostatistics. Oxford University Press, New York.
- Orús, R., Hernández-Pajares, M., Juan, J.M., Sanz, J., Garcia-Fernandez, M., 2002. Performance of different TEC models to provide GPS Ionospheric corrections. Journal of Atmospheric and Solar-Terrestrial Physics 64, 2055–2062.
- Samper, F.J., 1990. Geostatística: aplicaciones a la hidrología subterránea. Centro Internacional de Metodos Numericos (CINME), Barcelona.
- Stanislawski, I., Juchnikowski, G., Cander, Lj.R., 1996. Kriging method for instantaneous mapping at low and equatorial latitudes. Advances on Space Research 18 (6), 217–220.
- Stanislawski, I., Juchnikowski, G., Cander, Lj.R., Ciralo, L., Zbyszynski, Z., Swiatek, A., 2002. The kriging method of TEC instantaneous mapping. Advances on Space Research 29 (6), 945–948.
- Wessel, P., Smith, W.H.F., 2002. Generic Mapping Tools (GMT). <<http://gmt.soest.hawaii.edu/>>
- Wielgosz, P., Grejner-Brzezinska, D., Kashani, I., 2003. Regional ionosphere mapping with kriging and multi-quadratic methods. Journal of Global Positioning Systems 2 (1), 48–55.